

Exceptional points in coupled vortex-based spin-torque oscillatorsA. A. Matveev ^{*}*Kotel'nikov Institute of Radio-Engineering and Electronics of RAS, Moscow 125009, Russia,
and Moscow Institute of Physics and Technology (National Research University), Dolgoprudnyi, Moscow region 141701, Russia*A. R. Safin [†]*Kotel'nikov Institute of Radio-Engineering and Electronics of RAS, Moscow 125009, Russia
and National Research University Moscow Power Engineering Institute, Moscow 111250, Russia*S. A. Nikitov [‡]*Kotel'nikov Institute of Radio-Engineering and Electronics of RAS, Moscow 125009, Russia
and Moscow Institute of Physics and Technology (National Research University),
Dolgoprudnyi, Moscow region 141701, Russia* (Received 2 March 2023; revised 26 July 2023; accepted 3 November 2023; published 29 November 2023)

We theoretically study the linear and nonlinear dynamics of a system of mutually coupled magnetic vortices. We consider the excitation of vortex dynamics by both an external harmonic magnetic field and a spin-polarized current. The results based on the Thiele equations for the motion of coupled vortices are compared with the numerical integrations. Theoretical analysis shows that the appearance of the exceptional point corresponding to the coincidence of the normal modes of the system allows one to observe such effects as the death of amplitudes and parametric resonance. We propose a method for observing the effect of amplitude death in coupled magnetic vortices. In the investigated system, the emergence of exceptional points is controlled by the spin-polarized current and the strength of the coupling between vortices. Thus, possibilities are uncovered for the development of tunable spintronic devices.

DOI: [10.1103/PhysRevB.108.174443](https://doi.org/10.1103/PhysRevB.108.174443)**I. INTRODUCTION**

The study of nanoscale ferromagnets is of scientific interest due to the possibility of their application in spintronic devices, such as superdense data storage, magnetic logic elements, and spintronic oscillators [1–3]. The most promising spintronic nano-oscillators are those characterized by the vortex structure of the magnetization of the ferromagnetic layer [4]. It has been shown [2,5] that for such oscillators the highest level of output power of oscillations and a narrow width of the spectral line is achieved even without external magnetic field. Thus, the control of the magnetization dynamics in vortex nano-oscillators is possible both by applying an external magnetic field and by passing a spin-polarized current through the nanostructure [4,6]. Studies of magnetization dynamics for single vortices taking into account the nonlinearity are carried out [2,7,8]. Nonlinear effects such as frequency shift at resonance and the emergence of a limit cycle are investigated [4,9,10].

Nowadays, the phenomena arising in arrays of spintronic oscillators are most actively studied in connection with the tasks of constructing neuromorphic computing and Ising machines [2,11–13], as well as stable sources of oscillations

with the effect of power addition [14]. Various studies of linear and nonlinear regimes under the impact of external magnetic field and spin-polarized current have been carried out for a system of coupled vortex nano-oscillators [2]—in particular, the effects of mutual synchronization and multi-mode generation [15–19]. Nevertheless, in coupled oscillatory systems, with the help of a special choice of parameters, it is possible to achieve a state of the so-called “exceptional point” corresponding to the coincidence of the normal modes of the system [20–22]. In this state, it is possible to observe various effects (e.g., amplitude death and parametric resonance [23,24]). Currently, the possibilities of using dynamical behavior of different nature systems near the exceptional point for the tunable sensitive detector construction are being intensively investigated [25,26]. In particular, in spintronics, the latest research concerns the dynamic of waveguide systems in the vicinity of these states [20,21,27]. Recent theoretical and experimental research carried out for ferromagnets with vortex magnetization configuration showed the occurrence of the effect of amplitude death [23].

Several types of oscillations are possible in the system of two mutually coupled spin-torque vortex oscillators (STVOs). Self-oscillations occur when damping is compensated by pumping realized at the transmission of spin-polarized current through magnetic vortices. Driven oscillations are excited by an applied external harmonic magnetic field. In addition, the spintronic oscillator dynamics can be implemented by a special parametric impact [28]. In this paper, we consider the

^{*}maa.box@yandex.ru[†]arsafin@gmail.com[‡]nikitov@cplire.ru

as [4,19,23]

$$\mathbf{F}_{1,2} + \mathbf{G} \times \frac{d\mathbf{X}_{1,2}}{dt} + \widehat{\mathcal{D}}\alpha \frac{d\mathbf{X}_{1,2}}{dt} + \mathbf{T}_{STT_{1,2}} + \mathbf{F}_{c_{1,2}} + \mathbf{F}_{z_{1,2}} = 0. \quad (1)$$

Here $\mathbf{X}_{1,2} = (x_{1,2}, y_{1,2}, 0)$ are the displacements of the vortex cores from the centers of the disks; $\mathbf{F}_{1,2}$ are the potential forces; $\mathbf{G} = G\mathbf{e}_z$ is the gyrovector; $\widehat{\mathcal{D}}$ is the damping tensor; α is the Gilbert damping constant [33]; $\mathbf{F}_{c_{1,2}}$ are the coupling forces; $\mathbf{T}_{STT_{1,2}}$ are torques arising from the spin-polarized currents. In the thin-cylinder approximation, it is assumed that the damping tensor has only two nonzero components $\mathcal{D}_{xx} = \mathcal{D}_{yy} = \mathcal{D} = -[\pi M_s \mu_0 L \ln(R/l)]/\gamma$ [10,34]. Here M_s is the saturation magnetization; μ_0 is the magnetic constant; γ is the gyromagnetic ratio; l is the exchange length of the material [35]. For a vortex in a nanocylinder, the gyrovector module is calculated by the expression $G = -(2\pi M_s \mu_0 L)/\gamma$ [4,6]. It is shown [8] that for the CPP configuration spin-transfer torques are expressed as

$$\mathbf{T}_{STT_{1,2}} = J_{1,2} B \mathbf{e}_z \times \mathbf{X}_{1,2}, \quad (2)$$

where \mathbf{e}_z is the unit vector of the OZ axis; $B = \pi \hbar P/|e|$, where \hbar is the reduced Planck constant, e is the electron charge, and P is the spin polarization of the current.

The forces involved in equation (1) are calculated as gradients of the corresponding energies. The potential forces $\mathbf{F}_{1,2}$ arising from the fact that the exchange and magnetostatic energies are minimal when the vortex cores are in the centers of the disks are calculated using the expression [7]

$$\mathbf{F}_{1,2} = -\nabla_{1,2} \cdot \left(W_0 + \frac{\kappa}{2} |\mathbf{X}_{1,2}|^2 + \frac{\beta}{4} |\mathbf{X}_{1,2}|^4 \right). \quad (3)$$

Here operator $\nabla_{1,2}$ denotes differentiation with respect to the corresponding coordinates $\nabla_{1,2} \cdot W = (\partial W/\partial x_{1,2}, \partial W/\partial y_{1,2}, \partial W/\partial z_{1,2})$, where W is the scalar function; W_0 is the magnetic energy of one vortex when its core is located in the center of the disk. The exact value of W_0 is of no interest to dynamics because when taking the gradient in Eq. (3), it disappears. The stiffness coefficients $\kappa > 0$, $\beta > 0$ can be obtained from the experiment or micromagnetic simulation [10,36].

In [6] it is shown that the expressions for the Zeeman forces are written as

$$\mathbf{F}_{z_{1,2}} = -\nabla_{1,2} \cdot W_{z_{1,2}}(|\mathbf{X}_{1,2}|, \mathbf{H}_{1,2}) = A \mathbf{e}_z \times \mathbf{H}_{1,2}, \quad (4)$$

where $A = -\mu_0 M_s R L/2$ is the proportionality coefficient. In (4) the nonlinear term is not taken into account because it is much smaller than the nonlinearity in Eq. (3) [6].

The coupling in our model is symmetrical. This means that the coupling force acting on one vortex is proportional to the displacement relative to the equilibrium position of the second oscillator. This is a common situation for coupled oscillatory systems [19,24]. Then we can write

$$\mathbf{F}_{c_{1,2}} = -\nabla_{1,2} \cdot W_{\text{int}_{1,2}}(\mathbf{X}_{1,2}) = -\mu \mathbf{X}_{2,1}. \quad (5)$$

Here μ is coupling constant. Note that such an expression was used in [23] and coincides in form with the expression for the strength of the dipole coupling [15].

III. EXCEPTIONAL POINTS AND SELF-OSCILLATIONS

The appearance of exceptional points in the system of coupled oscillators is possible when the normal modes of the system coincide. Thus, in order to find the conditions for EP emergence, it is necessary to find these normal modes. For this from Eq. (1) we express the velocities of the vortex cores

$$\begin{pmatrix} \dot{x}_{1,2} \\ \dot{y}_{1,2} \end{pmatrix} = \begin{pmatrix} a\kappa x_{1,2} + a\beta(x_{1,2}^2 + y_{1,2}^2)x_{1,2} \\ a\kappa y_{1,2} + a\beta(x_{1,2}^2 + y_{1,2}^2)y_{1,2} \end{pmatrix} + \begin{pmatrix} -b\kappa y_{1,2} - b\beta(x_{1,2}^2 + y_{1,2}^2)y_{1,2} \\ b\kappa x_{1,2} + b\beta(x_{1,2}^2 + y_{1,2}^2)x_{1,2} \end{pmatrix} + \begin{pmatrix} -bBJ_{1,2}x_{1,2} + aBJ_{1,2}y_{1,2} \\ -bBJ_{1,2}y_{1,2} - aBJ_{1,2}x_{1,2} \end{pmatrix} + \begin{pmatrix} -AbH_{x,1,2} + AaH_{y,1,2} \\ -AbH_{y,1,2} - AaH_{x,1,2} \end{pmatrix} + \begin{pmatrix} \mu a x_{2,1} + b\mu y_{2,1} \\ \mu a y_{2,1} - b\mu x_{2,1} \end{pmatrix}, \quad (6)$$

where

$$a = \frac{\mathcal{D}\alpha}{(G^2 + (\mathcal{D}\alpha)^2)}, \quad b = \frac{G}{(G^2 + (\mathcal{D}\alpha)^2)}. \quad (7)$$

The system of four nonlinear equations (6) is cumbersome, so for simplicity we introduce complex amplitudes

$$c_{1,2} = x_{1,2} + i y_{1,2}. \quad (8)$$

Then without an external magnetic field the system of Thiele equations can be written as

$$\begin{aligned} \dot{c}_{1,2} + i(\omega_0 + \Delta\omega_{1,2} + Q_c|c_{1,2}|^2)c_{1,2} \\ + (\Gamma_0 + \Delta\Gamma_{1,2} + Q|c_{1,2}|^2)c_{1,2} = (i\Lambda_c + \Lambda)c_{2,1}. \end{aligned} \quad (9)$$

Here $\omega_0 = -b\kappa$, $\Delta\omega_{1,2} = -aBJ_{1,2}$, $\Gamma_0 = -a\kappa$, $\Delta\Gamma_{1,2} = bBJ_{1,2}$, $\Lambda_c = b\mu$, $\Lambda = a\mu$, $Q = -a\beta$, $Q_c = -b\beta$. The search for a solution of system (9) in the linear case $\beta = 0$ in the form $c_{1,2} = \exp(-i\lambda t)$ gives expressions for the normal modes of the system

$$\begin{aligned} \lambda_{\pm} = \frac{1}{2}(\omega_1 + \omega_2) - \frac{i}{2}(\Gamma_1 + \Gamma_2) \\ \pm i\sqrt{(i\omega + \Gamma)^2 + (\Lambda + i\Lambda_c)^2}, \end{aligned} \quad (10)$$

where $\omega = \frac{1}{2}(\Delta\omega_1 - \Delta\omega_2)$, $\Gamma = \frac{1}{2}(\Delta\Gamma_1 - \Delta\Gamma_2)$, $\omega_{1,2} = \omega_0 + \Delta\omega_{1,2}$, and $\Gamma_{1,2} = \Gamma_0 + \Delta\Gamma_{1,2}$.

In general, the problem under consideration is three-parameter, since we assume the possibility of changing the values of spin-polarized currents in each nanocylinder and the coupling constant between them. We start our analysis by fixing the coupling constant μ and finding the relations between the values of spin-polarized currents in nanocylinders at which the system reaches the exceptional point state $\lambda_- = \lambda_+$. Thus we get

$$J_2 = J_1 \pm \frac{2\mu}{B}. \quad (11)$$

Note that the obtained expressions (10) allow us to find not only exceptional points, but also areas of stability of the

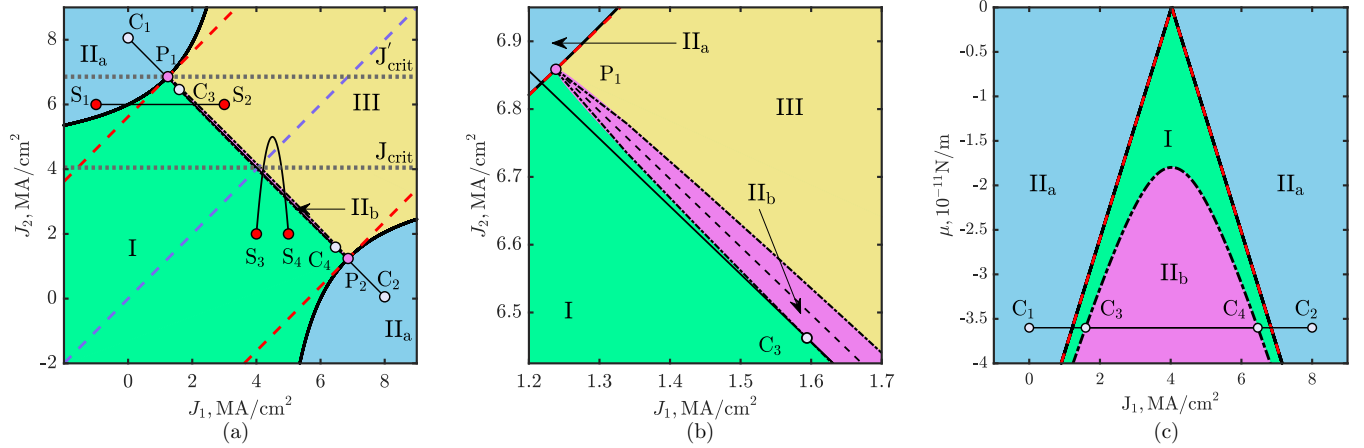


FIG. 2. Phase diagrams with indications of the areas of instability (II_a, II_b, III) and stability (I) of the linear regime. In region III, the imaginary parts of both normal modes are positive. In II_a, the inequality $\text{Im}[\lambda_+] > 0$ is fulfilled. In II_b, the inequality $\text{Im}[\lambda_-] > 0$ is fulfilled. (a) Phase diagram in the parameter plane (J_1, J_2). Solid black lines are plotted using (12), while dash-dotted black lines are plotted using (13). The red dashed line shows EPs. The purple dashed line on which $J_1 = J_2$ is the axis of symmetry of the diagram. Gray dotted lines show critical spin-polarized current densities J_{crit}, J'_{crit} . Line S_1S_2 illustrates a way to observe the effect of amplitude death near EP. The line S_3S_4 shows how one can switch between self-oscillation and steady linear mode without approaching EP. Line C_1C_2 plotted with help of (15) at $\delta = 0.005$. Points C_3, C_4 are the intersection of the lower boundary of the area II_a with the line C_1C_2 . The coupling constant is fixed $\mu = -3.6 \times 10^{-11}$ N/m. (b) The vicinity of point P_1 . Line C_1C_2 crosses the lower boundary of area II_b at point C_3 . (c) Phase diagram in the parameter surface (J_1, μ). Solid black lines are plotted using (16) and dash-dotted line corresponds to (17). The red dashed line shows EPs. Line C_1C_2 illustrates a way to observe the effect of amplitude death. The parameter δ is fixed $\delta = 0.005$.

linear oscillation regime. To do this, it is necessary to resolve inequalities $\text{Im}[\lambda_{\pm}] < 0$ since the solutions of (9) in the linear case have the form $c_{1,2} = \exp(-i\lambda t)$. It is shown that in such a system the instability of the linear regime leads to the Andronov-Hopf (supercritical) bifurcation, which means the birth of a limit cycle [2]. So, the obtained equations describing the boundaries of the sign change of the imaginary parts of the normal modes λ_{\pm} are written as

$$J_2^b = \frac{1}{bB} \left(ak + \frac{b^2 \mu^2}{ak - bB J_1} \right), \quad (12)$$

$$J_{2\pm}^b = \frac{1}{(a^2 + b^2)B} (B(a^2 - b^2)J_1 + 2abk \pm 2a\sqrt{(a^2 + b^2)\mu^2 - (ak - bB J_1)^2}). \quad (13)$$

The areas of stability and instability, boundaries, and exceptional points of the system are shown in Fig. 2(a). As one can see, the figure is symmetrical with respect to a line $J_1 = J_2$, which fully corresponds to the symmetry of the system since the indices 1 and 2 can be swapped.

To observe the effect of amplitude death near the EP, we fix the current density in the second nanocylinder J_2^* and increase the current density in the first oscillator starting from certain selected value J_1° and ending with a value J_1^* . The choice of these values should be made in such a way that the point $S_1 = (J_1^{\circ}, J_2^*)$ belongs to region II_a and the point $S_2 = (J_1^*, J_2^*)$ belongs to region III. In addition, it is necessary that the line S_1S_2 intersect region I. Then, when one moves from S_1 to S_2 , the system passes through area I, in which self-oscillations are impossible. This means that at the values of the current in the first nanocylinder that correspond to the location of the system in the region II_a or III, self-oscillations will be observed, and when the system enters region I, they will vanish. This is how the effect of amplitude death manifests itself.

All restrictions applied to a fixed current are mathematically equivalent to an inequality $J_{crit} < J_2^* < J'_{crit}$, where critical current densities are determined from expressions

$$J_{crit} = \frac{ak}{bB}, \quad J'_{crit} = \frac{1}{bB} (ak - b\mu). \quad (14)$$

The first of these equations can be obtained by taking the limit $\lim_{J_1 \rightarrow -\infty} J_2(J_1)$ using the relation (12). The second value J'_{crit} is found when searching for the intersection point of the lines (12) and (13). Besides, expressions for the stability boundaries of the linear regime allow us to find the width of the area of the vanishing of self-oscillations ΔJ_1 at a given value J_2^* as the difference between the current densities J_1 determined from Eqs. (12) and (13). So this width at different coupling coefficients is plotted in Fig. 3. As one can see, this area can be quite big or as small as necessary, depending on the fixed value of the current density J_2^* . However, the limitations of the used Thiele model should be taken into account. First of all, the model does not take into account the influence of temperature. Besides as shown in [4,8], the Thiele equation precisely describe the dynamics of a magnetic vortex with small deviations of the core from the equilibrium position. So, the observation of an arbitrarily small width ΔJ_1 can be limited by the influence of temperature not taken into account in Eq. (1). Moreover, with sufficiently large currents the vortex core can switch [2,4]. This means changing the sign of the parameter \mathcal{P} . The result will be a sign change in the pumping performed due to spin-polarized current. In this case, the excitation of self-oscillations in vortices will be possible only with a corresponding change in the direction of the density vector of the spin-polarized current. However, switching processes are beyond the scope of this paper.

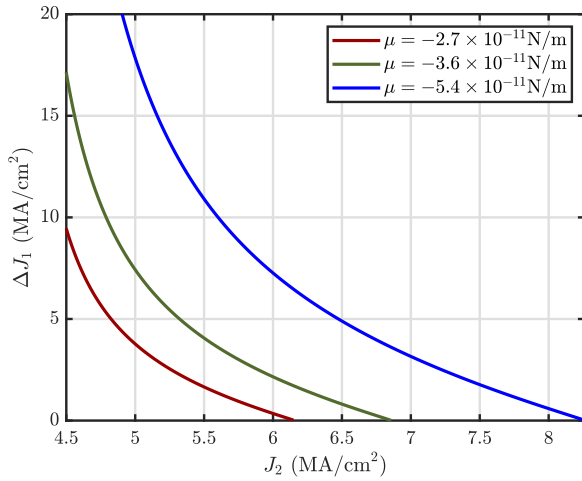


FIG. 3. Width ΔJ_1 of amplitude death region at various coupling constants μ .

There is another way to observe the phenomenon of amplitude death near the EP. It is interesting because it becomes possible to lead the system through two regions of the vanishing of self-oscillations. However, one can assume that there is an area of emergence of self-oscillations enclosed between these two regions. To implement this way, one can pull the system from the upper region Π_a to the lower Π_a while intersecting I and Π_b in Fig. 2(a). A line C_1C_2 parallel to the P_1P_2 satisfies these requirements. As one can see in Fig. 2(b), when the system moves along this line, area I will indeed be crossed. Then we can assume that the density J_2 varies depending on J_1 in accordance with the expression

$$J_2 = -J_1 + \frac{2a\kappa}{bB}(1 - \delta). \quad (15)$$

Here δ is the parameter. It is convenient to set the $J_2(J_1)$ in this form because at the exceptional point $\text{Im}[\lambda_+] = \text{Im}[\lambda_-] = -\delta\Gamma_0 = a\kappa\delta$. When the delta is equal to zero, the line specified by the formula (15) passes through the points P_1 and P_2 in Fig. 2(a). In this case, only regions Π_a and Π_b are intersected by this line. When the delta is equal to unity, the dependence (15) sets a line passing through $(0, 0)$ and parallel to P_1P_2 in Fig. 2(a). Such a line can only cross areas Π_b and I. It is possible to intersect all the necessary areas: Π_a , I, and Π_b with $\delta = 0.005$. Figure 2(a) is a phase diagram in the parameter plane (J_1, J_2) drawn at a fixed coupling coefficient. To study the influence of the choice of different μ on the observation of the effect of amplitude death by the method proposed in this paper, such a representation is inconvenient. Therefore, we redraw the phase diagram by selecting the parameters (J_1, μ) . To find the stability boundaries in this case, it is necessary to solve the equations $\text{Im}[\lambda_{\pm}] = 0$ with respect to μ . So the obtained relations have the form

$$\mu_{1\pm}^b = \pm \frac{1}{b} \sqrt{a\kappa(2\delta - 1) + bBJ_1}(bBJ_1 - a\kappa), \quad (16)$$

$$\mu_{2\pm}^b = \pm \frac{1}{b} \{[(\delta - 1)^2 a^2 + b^2 \delta^2] \kappa^2 + 2Bab(\delta - 1)\kappa J_1 + (bBJ_1)^2\}^{\frac{1}{2}}. \quad (17)$$

The equations for determining EPs are found from expressions (11) and (15),

$$\mu = \pm \frac{1}{b} [bB J_1 + (1 - \delta)a\kappa]. \quad (18)$$

The phase diagram of the system in the parameter surface (J_1, μ) is shown in Fig. 2(c). Due to the symmetry of the coupling, we draw only half-plane $\mu < 0$. There is no need to depict a half-plane $\mu > 0$ because it is a mirror image of Fig. 2(c). Note that although the EPs defined by expression (18) are close enough to the boundary plotted using Eq. (16), they do not coincide.

To observe the effect of amplitude death, one can move along line C_1C_2 drawn at a constant μ^* . When the system parameters belong to regions Π_a and Π_b , self-oscillations are possible, while in region I, self-oscillations vanish. Since here we are interested in observing two areas of amplitude death, we find the critical coupling constant μ_{crit}^* at which line C_1C_2 becomes tangent to the boundary (17). So the obtained equation has the simple form

$$\mu_{\text{crit}}^* = \pm \kappa \delta. \quad (19)$$

For any $|\mu| < |\mu_{\text{crit}}^*|$, there is only one region of amplitude death. Note that when the coupling coefficient is sufficiently close to zero, all the equations obtained break down to correctly describe the behavior of the system, which is normal since the oscillators cease to be coupled.

The length of the segment C_3C_4 in Fig. 2(c) corresponds to the width $\Delta J_1'$ of the area of emergence of self-oscillations. This value can be found by substituting the coupling constant $\mu = \mu^*$ into expression (17) and solving the resulting quadratic equation with respect to the current density in the first nanocylinder and finding the difference between the roots. So one can write

$$\Delta J_1' = \frac{2}{B} \sqrt{\mu^{*2} - \delta^2 \kappa^2}. \quad (20)$$

It is clear that when the coupling constant approaches its critical value, the width becomes sufficiently close to zero. It should also be taken into account that a sufficiently high value μ^* required to achieve a larger $\Delta J_1'$ can lead to the destruction of the vortex structure in nanocylinders since in this case the amplitudes of the coupling fields $H_{c1,2}$ become big enough.

Note that it is possible to achieve the vanishing of self-oscillations in the system under study without considering the dynamics near exceptional points—for example, if one moves the system in the phase diagram shown in Fig. 2(a) along line S_3S_4 . As one can see, there are no self-oscillations at points S_3 and S_4 located in area I, while they occur in area III. However, to implement such an opportunity, a nonlinear dependence $J_2(J_1)$ is required, while to observe the effect of amplitude death near EPs, a linear dependence like (15) or fixation of one of the currents is sufficient.

Based on the methods described in this section for observing the effect of amplitude death, it is possible to design sensitive tunable sensors. The sensitivity of normal modes near exceptional points makes it possible to observe a change in the oscillation mode of the system when passing through the vicinity of these points in the space of parameters. Since the vortex oscillation mode can be converted into an electrical

signal using TMR [23], the output signal of the sensor will be extremely sensitive to changes in the input spin-polarized currents J_1 , J_2 . The width of the area of changing of the output signal as shown in this section is controlled by the coupling coefficient, which can be adjusted using amplifiers (see Sec. II). However, self-oscillations are not the only types of oscillations that can be excited in a system of coupled magnetic vortices. The application of an external harmonic magnetic field excites driven oscillations. This allows us to investigate the resonant properties of the system.

IV. EXCEPTIONAL POINTS IN NONLINEAR RESONANCE

Let us proceed to the study of the resonant properties of the system. In this section we describe the resonance that occurs in the system when an external harmonic magnetic field is applied. Such frequency response is a selective reaction of a system of coupled oscillators to this external impact. Determining the influence of the EP emergence on this selectivity may begin with finding resonant frequencies. Then the terms corresponding to this external magnetic field should be included in Eq. (9). We assume a harmonic influence; therefore they have the form $H_{1,2} \exp(-i\Omega t)$. Here the complex amplitudes of the external field are calculated by the formulas $H_{1,2} = A(aH_{y,1,2} - bH_{x,1,2}) + iA(aH_{x,1,2} + bH_{y,1,2})$. To derive the resonant frequencies and amplitudes in the linear regime of the oscillations of the vortex cores, we write down Eq. (9) for $c_{1,2}$ under the condition $\beta = 0$ taking into account external fields

$$\begin{aligned} \dot{c}_{1,2} + i(\omega_0 + \Delta\omega_{1,2})c_{1,2} + (\Gamma_0 + \Delta\Gamma_{1,2})c_{1,2} \\ = (i\Lambda_c + \Lambda)c_{2,1} + H_{1,2} \exp(-i\Omega t) \end{aligned} \quad (21)$$

and search for a solution in the form $c_{1,2} = r_{1,2} \exp(-i\Omega t)$. The solution of the system of linear equations obtained in this case is given by

$$r_{1,2} = \frac{(i\Lambda_c + \Lambda)H_{2,1} + [i(\omega_{1,2} - \Omega) + \Gamma_{1,2}]H_{1,2}}{[i(\omega_1 - \Omega) + \Gamma_1][i(\omega_2 - \Omega) + \Gamma_2] + (i\Lambda_c + \Lambda)^2}. \quad (22)$$

In the linear case, there are resonant frequencies Ω_{res} among the extremum points of the amplitude modules $|r_{1,2}|$. However, solving the equations $\partial|r_{1,2}|/\partial\Omega = 0$ is a complicated task due to the fact that they have the fifth order relative to the desired extremum points. The general analytical solution of such equations is unknown. Therefore, we use simplifications. In the magnetic vortices under consideration, the values of the gyrovectore module $|G|$ and the module of the component of the damping tensor $|\mathcal{D}|$ are approximately of the same order, although the formula for the coefficient a (7) includes a small Gilbert damping constant α in the numerator. Hence the value of the ratio $|a|/|b| = \mathcal{D}\alpha/G \approx 0.01$ allows us to disregard the terms $\Delta\omega_{1,2}$ and Λ . Note that since the effect of the spin-polarized current on the frequency is proportional to its density $\Delta\omega_{1,2} = -aB J_{1,2}$, neglecting the $\Delta\omega_{1,2}$ is possible only in a certain range $J_{1,2}$. In addition, we consider cases when an external harmonic magnetic field is applied only to the one of the nanocylinders.

Taking into account all the simplifications made, the solutions of the equation $\partial|r_{1,2}|/\partial\Omega = 0$ are written as

$$\Omega_{01} = \Omega_{02} = \omega_0, \quad (23)$$

$$\Omega_{1\pm}^{H_1} = \omega_0 \pm \sqrt{|\Lambda_c| \sqrt{\Lambda_c^2 + 2\Gamma_1\Gamma_2 + 2\Gamma_2^2} - \Gamma_2^2}, \quad (24)$$

$$\Omega_{2\pm}^{H_2} = \Omega_{2\pm}^{H_1} = \omega_0 \pm \sqrt{\Lambda_c^2 - \frac{1}{2}(\Gamma_1^2 + \Gamma_2^2)}, \quad (25)$$

$$\Omega_{2\pm}^{H_2} = \omega_0 \pm \sqrt{|\Lambda_c| \sqrt{\Lambda_c^2 + 2\Gamma_1\Gamma_2 + 2\Gamma_1^2} - \Gamma_1^2}. \quad (26)$$

Here $\Omega_{k\pm}^{H_m}$ denotes the frequency at which the amplitude $|r_k|$ is maximal under the condition $H_m \neq 0$. So, if we set $H_m \neq 0$ in one nanocylinder and the field in another is equal to zero, then if $\Omega_{k\pm}^{H_m}$ are real, then they correspond to resonant frequencies, while expression (23) determines the local minimum on the frequency response. If $\Omega_{k\pm}^{H_m}$ turn out to be complex, then the frequency ω_0 is the only resonant frequency. Thus, the condition for the existence of a single resonant peak on the frequency response is the complexity of the frequencies $\Omega_{k\pm}^{H_m}$. The heights of these resonant peaks can be found by substituting $\Omega_{k\pm}^{H_m}$ or ω_0 into the expressions (22) and calculating the amplitude modules $|r_{1,2}|$. The formulas obtained in this case are cumbersome, but the calculation with their help is not complicated.

The resonant frequencies in general do not coincide with the eigenfrequencies with appropriate simplifications $\text{Re}[\lambda_{\pm}]$. If we assume that the coupling is greater than damping or pumping in each of the nanocylinders $\Gamma_{1,2} \ll \Lambda_c$ then $\text{Re}[\lambda_{\pm}] = \Omega_{k\pm}^{H_m}$ holds. This is a common situation for oscillators when damping leads to the fact that there is no resonance at eigenfrequencies [37]. Thus, the EP state does not correspond to the degeneration of two peaks into one at the frequency response, as is observed in waveguide systems [21].

To study the nonlinear resonance, we performed numerical integration of the Thiele equations (6). The results are shown in Figs. 4(a) and 4(b). For calculations, we chose a case when the current in the second nanocylinder is fixed. With the selected density $J_2 = 5 \text{ MA/cm}^2$, the switch to the self-oscillating mode is possible at both $J_1 = -4.3 \text{ MA/cm}^2$ and $J_1 = 3.0 \text{ MA/cm}^2$. Therefore, the left and right boundaries of Figs. 4(a) and 4(b) correspond to the loss of stability in the linear regime. So as the system approaches the boundary of the switch to the self-oscillating mode, the resonant amplitude increases. This happens because the Andronov-Hopf bifurcation in the system under study means exact compensation of damping by means of spin-polarized current. And it is known that a resonator with a small damping has a large amplitude in resonance.

With small deviations of the vortex cores from the equilibrium positions, the numerically calculated amplitudes coincide with those determined analytically. This indicates that the used simplifications are acceptable for describing the amplitudes. As one can see, the nonlinearity leads to a significant decrease in the resonant amplitude in comparison with the linear case. However, in the calculated case, the nonlinearity did not affect the condition of the existence of two peaks on the frequency response. Figure 4 also shows that the resonance in the region where there is only one peak on the frequency

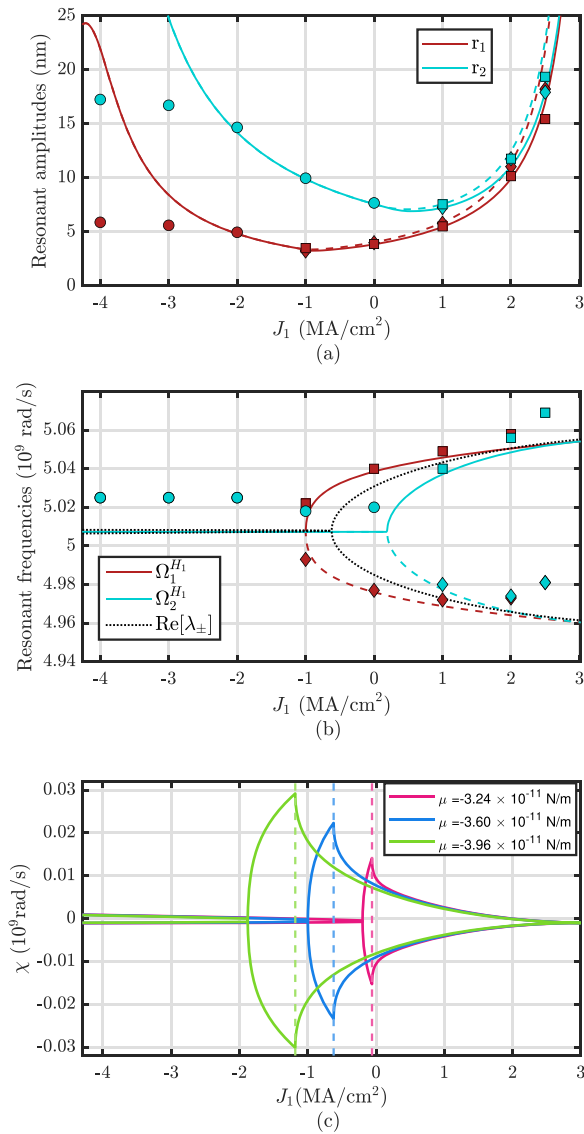


FIG. 4. Dependencies of resonant amplitudes (a), frequencies (b), and frequency shift χ (c) of coupled vortices on the J_1 . The external harmonic magnetic field applied to the first vortex is directed along the OY axis and has an amplitude $H_{y1} = 500$ A/m. The current density in the second nanocylinder is fixed $J_2 = 5$ MA/cm². (a), (b) Coupling constant $\mu = -3.6 \times 10^{-11}$ N/m. Solid and dashed lines denote analytically obtained dependencies for the linear regime. Squares and diamonds denote the results obtained by numerical integration of the Thiele equations. The dashed lines and diamonds refer to the low-frequency peak on the frequency response while the solid lines and squares refer to the high-frequency peak. If there is one peak then a circle is drawn for numerical results. The color according to the legend shows which of the nanocylinders the results belong to. Dashed black lines refer to eigenfrequencies. (c) Solid lines are plotted using $\chi = \Omega_{1\pm}^{H_1} - \text{Re}[\lambda_{\pm}]$. Dashed vertical lines are drawn at the J_1 corresponding to the state of the exceptional point. The color according to the legend shows which coefficient of coupling the result refers to.

response does not occur at the frequency ω_0 as follows from the formula (23). This is due to the fact that we have neglected

the term $\Delta\omega_{1,2}$. In the case when the influence of currents is taken into account (24), (25) and the deviations of the vortex cores from their equilibrium positions are small, as for example with current densities $J_1 = -1$ to 1 MA/cm² in the first nanocylinder, the coincidence of numerical calculations and analytical results is observed. The nonlinearity determines the shift of the resonant frequency to the high-frequency region, as it is for one nanocylinder and is determined by the β sign [2,10].

In order to show the sensitivity of the system of coupled magnetic vortices in the case under study, it is possible to depict the shift of resonant frequencies relative to the eigenfrequencies $\chi = \Omega_{1\pm}^{H_1} - \text{Re}[\lambda_{\pm}]$. As one can see from Fig. 4(c), the dependence $\chi(J_1)$ changes dramatically when passing through an exceptional point. Thus, if the system is in an exceptional point state $J_1 = J_1^{\text{EP}}$, even a small perturbation of the spin-polarized current density $J_1 = J_1^{\text{EP}} + \Delta_p J_1$ will significantly change the frequency shift χ . Here J_1^{EP} can be found with help of (11), and perturbation $\Delta_p J_1$ may have a different nature. It may appear due to thermal effects or it may be a signal that needs to be registered. The control of the coupling coefficient in this case allows one to adjust J_1^{EP} .

V. PARAMETRIC RESONANCE

In addition to the resonance described in the previous section, when an external harmonic magnetic field is applied, a parametric resonance can also be obtained in coupled vortices. In this section, we refer to parametric resonance as the instability of the linear regime arising in the case of small oscillations of one of the parameters of the system. From the point of view of practical applications, it makes sense to consider only small harmonic perturbations in the densities of spin-polarized currents or in the coupling between oscillators, since it is impossible to give such a perturbation to other system parameters, e.g., material parameters and sizes of the nanocylinders.

Let us consider that the density of the spin-polarized current oscillates with a small amplitude around a given stationary value $J_1(t) = J_{01} + j \cos(\Omega t)$. The value J_{01} , the constant current density in the second nanocylinder J_2 , and the coupling constant μ are such that the system is in the state of an exceptional point. So we can consider the equation $J_{01} = J_2 + 2\mu/B$ is fulfilled. Besides we assume that $\beta = 0$ and neglect $\Delta\omega_{1,2}$ and Λ for the reasons explained in Sec. IV. Then Eq. (9) take the form

$$\dot{c}_1 + i\omega_0 c_1 + [\Gamma_0 + \Delta\Gamma_{01} + \eta(t)]c_1 = i\Lambda_c c_2, \quad (27)$$

$$\dot{c}_2 + i\omega_0 c_2 + (\Gamma_0 + \Delta\Gamma_2)c_2 = i\Lambda_c c_1. \quad (28)$$

Here $\Delta\Gamma_{01} = -bBJ_{01}$, $\eta(t) = -bBj \cos(\Omega t) = \eta_0 \cos(\Omega t)$. Analyzing Eqs. (27), (28) we obtain an expression for the boundary frequency of parametric resonance (see Appendix A for the details)

$$\Omega_b^2 = -4\delta^2 \Gamma_0^2 + \frac{1}{2} \eta_0 \sqrt{16\Gamma_0^2 \delta^2 + 16\Lambda_c^2 - \eta_0^2}. \quad (29)$$

Parametric resonance is observed for all frequencies $\Omega < \Omega_b$. To verify this statement, numerical integrations of the Thiele equations were carried out. The results are shown in

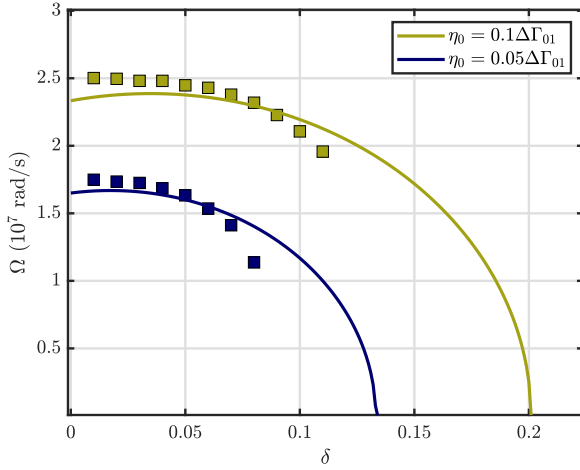


FIG. 5. The boundary frequencies of parametric resonance with oscillations of the spin-polarized current density $J_1 = J_{01} + \eta_0 \cos(\Omega t)$ depending on δ . Solid lines are plotted using (29). Squares mark the results of numerical integration of Thiele equations. The color according to the legend indicates which parameter η_0 the results relate to. Coupling constant $\mu = -7.15 \times 10^{-11}$ N/m.

Fig. 5. As one can see the analytically determined stability boundary only approximately corresponds to the calculated one. Note that we did not expect exact convergence because simplifications were applied. However, the obtained condition $\Omega < \Omega_b$ can be explained. If the additional pumping due to the oscillating part has frequency $\Omega < \Omega_b$, then the inertia of the system does not allow magnetic vortices to react to this small parametric influence. If the frequency is not too high, then the equations of motion of the cores of magnetic vortices cannot be averaged over the period $T = 2\pi/\Omega$ and additional pumping leads to instability.

There is another way to implement parametric resonance in a system of coupled magnetic vortices. We assume that it is possible to add a small oscillating part to the coupling current $I_{c_{2 \rightarrow 1}}$. This leads to the fact that the coupling ceases to be symmetrical and the first nanocylinder is additionally affected by the oscillating magnetic field. Mathematically, this means oscillating the coupling coefficient $\mu(t) = \mu_0[1 + \xi_0 \cos(\Omega t)]$ in the equations for the motion of the core of the first vortex. So the equations for complex amplitudes for the linear regime can be written as

$$\dot{c}_1 + i\omega_0 c_1 + \Gamma_1 c_1 = i\Lambda_c [1 + \xi_0 \cos(\Omega t)] c_2, \quad (30)$$

$$\dot{c}_2 + i\omega_0 c_2 + \Gamma_2 c_2 = i\Lambda_c c_1. \quad (31)$$

By investigating the solutions of this equations, one can obtain an expression for the boundary frequency of parametric resonance (see Appendix B for the details)

$$\Omega_b^2 = 2\xi_0 \Lambda_c^2 - 4\Gamma_0^2 \delta^2. \quad (32)$$

If the oscillation frequency of the coupling constant turns out to be less than the boundary (32) then the linear regime is unstable. We performed numerical integrations of Thiele equations to estimate the accuracy of determining the boundary frequency in this case. The results are shown in Fig. 6. As expected according to analytical calculations, the threshold

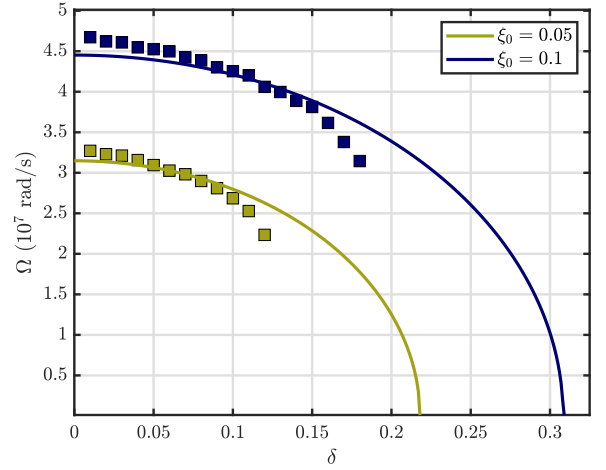


FIG. 6. The boundary frequencies of parametric resonance with oscillations of coupling coefficient $\mu = \mu_0 + \xi_0 \cos(\Omega t)$ in first nanocylinder depending on δ . Solid lines are plotted using (32). Squares mark the results of numerical integration of Thiele equations. The color according to the legend indicates which parameter ξ_0 the results relate to. Coupling constant $\mu_0 = -7.15 \times 10^{-11}$ N/m.

frequency decreases with increasing δ . However, numerical calculations have shown that the dependence has a sharper character than the theory developed in this work predicts.

With the parameters used in this section, the threshold oscillation frequencies fall into the high-frequency band. To increase Ω_b , it is necessary to reduce the damping of the material from which the nanocylinders are made, increase the coupling constant, or increase the oscillation amplitude ξ_0 and η_0 . However, it is not possible to increase the frequency by several orders of magnitude. The Gilbert damping in permalloy does not vary widely [33]. Increasing μ by several orders of magnitude can lead to remagnetization of nanocylinders as the coupling fields $\mathbf{H}_{c_{1,2}}$ become large. Setting a high level of oscillations leads to the fact that the expressions obtained here cease to be correct. This limitation arises from the fact that we assumed that the amplitudes of parametric impacts are low $\xi_0 \ll 1$, $\eta_0 \ll \Delta \Gamma_{01}$.

Note that in this section, when analyzing the dynamics of vortices, it was assumed that the densities of spin-polarized currents and the coupling coefficient were selected in such a way that the system is in the state of an exceptional point. Thus, the presence of the boundary frequency of instability of the linear regime indicates the sensitivity of the system to the frequency of the parametric impact. It turns out that if one use TMR to register the mode of vortex oscillations, then one can get a sensor that registers the frequency transition of the input signal through Ω_b . This frequency can be controlled by selecting a parameter δ .

VI. CONCLUSION

In summary, we have presented the results of the investigation of the dynamics of coupled magnetic vortices near exceptional points under the influence of spin-polarized current in the CPP configuration and applied external harmonic magnetic field. We described the amplitude death and found critical currents to observe this effect at a fixed current

density in one of the STVO. Moreover, a method of observing this effect near exceptional points is proposed in this paper. A critical coupling constant is defined for this case. We demonstrate that the EPs in the general case do not correspond to the transition of the system to a state with a single resonant frequency. The conditions of such a transition are defined. In addition, the role of nonlinearities in resonance is taken into account. It consists in that the stiffness coefficient β determines the nonlinear frequency shift to the high-frequency region as well as the decrease of the resonant amplitude. We show that pumping oscillations in one of the STVOs lead to parametric instability. The boundary oscillation frequency of the spin-polarized current is determined for this case. Moreover, we have shown the possibility of implementing parametric resonance with coupling oscillations and found expressions for determining the stability boundaries.

The presented results reveal the potential of EPs in coupled magnetic systems with vortex ground states. The parametric nature of the effects occurring near EPs will make it possible to design sensitive detectors controlled by spin-polarized current using the investigated system.

ACKNOWLEDGMENTS

The study of amplitude death was supported by the Russian Science Foundation through Grant No. 19-19-0607. Investigation of the resonance of a system of coupled magnetic vortices when an external harmonic magnetic field is applied was supported by grant from the Government of the Russian Federation for state support of scientific research conducted under the guidance of leading scientists in Russian higher education institutions, research institutions, and state centers of the Russian Federation (Project No. 075-15-2022-1098). Parametric resonance research was supported by the Russian Science Foundation through Grant No. 21-79-10396.

APPENDIX A: DERIVATION OF THE BOUNDARY FREQUENCY OF PARAMETRIC RESONANCE FOR SMALL OSCILLATIONS OF SPIN-POLARIZED CURRENT

We begin our analysis of the dynamics of magnetic vortices by searching for solutions of Eqs. (27), (28) in the form $c_{1,2} = r_{1,2}(t) \exp(-i\lambda_{EP}t)$, where $\lambda_{EP} = \omega_0 - i(\Gamma_1 + \Gamma_2)/2$. This can be done because we consider the dynamics near the EP. Thus the system of equations (27), (28) is equivalent to

$$\dot{r}_1 + [\Gamma + \eta(t)]r_1 = i\Lambda_c r_2, \quad (\text{A1})$$

$$\dot{r}_2 - \Gamma r_2 = i\Lambda_c r_1. \quad (\text{A2})$$

We reduce the obtained system of two differential equations of the first order to one equation of the second order

$$\ddot{r}_2 + \eta(t)\dot{r}_2 - \Gamma\eta(t)r_2 = 0. \quad (\text{A3})$$

We introduce a new variable $U(t)$ as $r_2(t) = U(t) \exp[-\eta_0 \sin(t)/(2\Omega)]$. Then one can write

$$\ddot{U} + [\Theta_0 + 2\Theta(t)]U = 0, \quad (\text{A4})$$

where $\Theta(t) = \Theta_s \sin(\Omega t) + \Theta_c \cos(\Omega t) + \Theta_{2c} \cos(2\Omega t)$; $\Theta_s = \eta_0 \Omega/4$; $\Theta_c = -\Gamma \eta_0/2$; $\Theta_{2c} = -\eta_0^2/16$; $\Theta_0 = -\eta_0^2/8$. The obtained equation is a Hill type equation [38]. In the

case under consideration, we are interested in determining the areas of instability under parametric impact. Therefore, we do not search for the exact type of solution. It is enough to substitute $U(t) = \exp(st) \sin(\Omega t/2 - \sigma)$ into Eq. (A4) and determine the increase parameter s as is done for the generalized Hill equation [38]. So equating the coefficients at $\sin(\Omega t/2)$ and $\cos(\Omega t/2)$ to zero we get

$$s \frac{\Omega}{2} = \Theta_c \sin(2\sigma) - \Theta_s \cos(2\sigma), \quad (\text{A5})$$

$$\Theta_0 = \left(\frac{\Omega}{2}\right)^2 - s^2 + \Theta_s \sin(2\sigma) + \Theta_c \cos(2\sigma). \quad (\text{A6})$$

Here we neglect the overtones with frequencies $3\Omega/2$, $5\Omega/2$ because the equations can be averaged over their periods. We solve the system (A5), (A6) and get an expression for the parameter s

$$s = \pm \sqrt{-\Theta_0 - \frac{\Omega^2}{4} \pm \sqrt{\Omega^2 \Theta_0 + \Theta_s^2 + \Theta_c^2}}. \quad (\text{A7})$$

Strictly speaking, four solutions have been obtained, but we are interested in only one for which the inequality $s > 0$ can be fulfilled. Therefore, both plus signs should be selected in Eq. (A7).

We are looking for such spin-polarized current densities J_{10} , J_2 , j and coupling constant μ at which the linear oscillation regime will be unstable. To achieve this, it is necessary to comply with the condition $s + \text{Re}[-i\lambda_{EP}] > 0$. This condition is obtained by taking into account the substitutions made $c_2 \rightarrow r_2 \rightarrow U$. Note that the exponent in the expression $r_2(t) = U(t) \exp[-\eta_0 \sin(t)/(2\Omega)]$ is not taken into consideration here because it cannot lead to instability. However, the frequency of small oscillations of the spin-polarized current Ω is in the denominator of the fraction $-\eta_0 \sin(t)/(2\Omega)$, which means that the applied formalism gives correct results not at too low frequencies.

For convenience, we assume that the densities J_{01} and J_2 are connected by the relation

$$J_{01} = \frac{1}{bB} [a\kappa(1 - \delta) + b\mu], \quad (\text{A8})$$

$$J_2 = \frac{1}{bB} [a\kappa(1 - \delta) - b\mu]. \quad (\text{A9})$$

Thus, δ determines the values of currents in nanocylinders with a fixed coupling. Then from $s + \text{Re}[-i\lambda_{EP}] > 0$ we get the stability boundary

$$\Omega_b^2 = -4\delta^2 \Gamma_0^2 + \frac{1}{2} \eta \sqrt{16\Gamma_0^2 \delta^2 + 16\Lambda_c^2 - \eta^2}. \quad (\text{A10})$$

Parametric resonance is observed for all frequencies $\Omega < \Omega_b$.

APPENDIX B: DERIVATION OF THE BOUNDARY FREQUENCY OF PARAMETRIC RESONANCE FOR SMALL OSCILLATIONS IN COUPLING

Let us consider the case when the system is in the state of an EP, which means that the current densities can be calculated using formulas (A8), (A9) with substitutions $\mu \rightarrow \mu_0$, $J_{01} \rightarrow J_1$. The equations for complex amplitudes for the linear regime

and using the possibility of neglecting the values $\Delta\omega_{1,2}$ and Λ can be written as

$$\dot{c}_1 + i\omega_0 c_1 + \Gamma_1 c_1 = i\Lambda_c [1 + \xi_0 \cos(\Omega t)] c_2, \quad (\text{B1})$$

$$\dot{c}_2 + i\omega_0 c_2 + \Gamma_2 c_2 = i\Lambda_c c_1. \quad (\text{B2})$$

We apply transformations similar to those used in finding the stability boundaries of the linear regime in the case when we assumed small oscillations of the spin-polarized current density in the first nanocylinder. Then when searching for a solution in the form $c_{1,2} = r_{1,2}(t) \exp(-i\lambda_{EP}t)$ we get

$$\dot{r}_1 + \Gamma r_1 = i\Lambda_c [1 + \xi_0 \cos(\Omega t)] r_2, \quad (\text{B3})$$

$$\dot{r}_2 - \Gamma r_2 = i\Lambda_c r_1. \quad (\text{B4})$$

We reduce this system to the Hill parametric oscillator equation

$$\ddot{r}_2 + \Lambda_c^2 \xi_0 \cos(\Omega t) r_2 = 0. \quad (\text{B5})$$

Substituting $r_2 = \exp(st) \sin(\Omega t/2 - \sigma)$ in this equation we get a system

$$\left(\frac{\xi_0 \Lambda_c^2}{2} + s^2 - \frac{\Omega^2}{4} \right) \sin(\sigma) - s\Omega \cos(\sigma) = 0, \quad (\text{B6})$$

$$\left(-\frac{\xi_0 \Lambda_c^2}{2} + s^2 - \frac{\Omega^2}{4} \right) \cos(\sigma) + s\Omega \sin(\sigma) = 0. \quad (\text{B7})$$

Here the overtones with frequency $3\Omega/2$ are not taken into account. The solution we are interested in has the form

$$s = \frac{1}{2} \sqrt{2\xi_0 \Lambda_c^2 - \Omega^2}. \quad (\text{B8})$$

Due to the replacement made $c_2 \rightarrow r_2$, the instability condition of the linear regime remains $s + \text{Re}[-i\lambda_{EP}] > 0$. So one can write

$$\Omega_b^2 = 2\xi_0 \Lambda_c^2 - 4\Gamma_0^2 \delta^2. \quad (\text{B9})$$

Parametric resonance is observed for all frequencies $\Omega < \Omega_b$.

-
- [1] T. Yamaguchi, N. Akashi, K. Nakajima, H. Kubota, S. Tsunegi, and T. Taniguchi, Step-like dependence of memory function on pulse width in spintronics reservoir computing, *Sci. Rep.* **10**, 19536 (2020).
- [2] K. Zvezdin and E. Ekomasov, Spin currents and nonlinear dynamics of vortex spin torque nano-oscillators, *Phys. Metals Metallogr.* **123**, 201 (2022).
- [3] S. Bohlens, B. Krüger, A. Drews, M. Bolte, G. Meier, and D. Pfannkuche, Current controlled random-access memory based on magnetic vortex handedness, *Appl. Phys. Lett.* **93**, 142508 (2008).
- [4] Y. B. Gaididei, V. P. Kravchuk, and D. D. Sheka, Magnetic vortex dynamics induced by an electrical current, *Int. J. Quantum Chem.* **110**, 83 (2010).
- [5] F. Sanches, V. Tiberkevich, K. Y. Guslienko, J. Sinha, M. Hayashi, O. Prokopenko, and A. Slavin, Current-driven gyrotropic mode of a magnetic vortex as a nonisochronous auto-oscillator, *Phys. Rev. B* **89**, 140410(R) (2014).
- [6] K. Y. Guslienko, R. H. Heredero, and O. Chubykalo-Fesenko, Nonlinear gyrotropic vortex dynamics in ferromagnetic dots, *Phys. Rev. B* **82**, 014402 (2010).
- [7] A. Drews, B. Krüger, G. Selke, T. Kamionka, A. Vogel, M. Martens, U. Merkt, D. Möller, and G. Meier, Nonlinear magnetic vortex gyration, *Phys. Rev. B* **85**, 144417 (2012).
- [8] A. V. Khvalkovskiy, J. Grollier, A. Dussaux, K. A. Zvezdin, and V. Cros, Vortex oscillations induced by spin-polarized current in a magnetic nanopillar: Analytical versus micromagnetic calculations, *Phys. Rev. B* **80**, 140401(R) (2009).
- [9] A. Dussaux, A. V. Khvalkovskiy, P. Bortolotti, J. Grollier, V. Cros, and A. Fert, Field dependence of spin-transfer-induced vortex dynamics in the nonlinear regime, *Phys. Rev. B* **86**, 014402 (2012).
- [10] A. A. Matveev, A. R. Safin, and S. A. Nikitov, Nonlinear resonance upon the excitation of a magnetic nanocylinder by a spin-polarized current, *JETP Lett.* **116**, 456 (2022).
- [11] J. Zhou and J. Chen, Prospect of spintronics in neuromorphic computing, *Adv. Electron. Mater.* **7**, 2100465 (2021).
- [12] M. Romera, P. Talatchian, S. Tsunegi, F. A. Araujo, V. Cros, P. Bortolotti, J. Trastoy, K. Yakushiji, A. Fukushima, H. Kubota, S. Yuasa, M. Ernout, D. Vodenicarevic, T. Hirtzlin, N. Locatelli, D. Querlioz, and J. Grollier, Vowel recognition with four coupled spin-torque nano-oscillators, *Nature (London)* **563**, 230 (2018).
- [13] A. Mondal and A. Srivastava, Ising-FPGA: A spintronics-based reconfigurable Ising model solver, *ACM Trans. Des. Autom. Electron. Syst.* **26**, 27 (2020).
- [14] R. Sharma, R. Mishra, T. Ngo, Y.-X. Guo, S. Fukami, H. Sato, H. Ohno, and H. Yang, Electrically connected spin-torque oscillators array for 2.4 GHz WiFi band transmission and energy harvesting, *Nat. Commun.* **12**, 2924 (2021).
- [15] A. D. Belanovsky, N. Locatelli, P. N. Skirdkov, F. Abreu Araujo, J. Grollier, K. A. Zvezdin, V. Cros, and A. K. Zvezdin, Phase locking dynamics of dipolarly coupled vortex-based spin transfer oscillators, *Phys. Rev. B* **85**, 100409(R) (2012).
- [16] R. Lebrun, J. Grollier, F. Abreu Araujo, P. Bortolotti, V. Cros, A. Hamadeh, X. de Milly, Y. Li, G. de Loubens, O. Klein, S. Tsunegi, H. Kubota, K. Yakushiji, A. Fukushima, and S. Yuasa, Driven energy transfer between coupled modes in spin-torque oscillators, *Phys. Rev. B* **95**, 134444 (2017).
- [17] R. Lebrun, N. Locatelli, S. Tsunegi, J. Grollier, V. Cros, F. Abreu Araujo, H. Kubota, K. Yakushiji, A. Fukushima, and S. Yuasa, Nonlinear behavior and mode coupling in spin-transfer nano-oscillators, *Phys. Rev. Appl.* **2**, 061001(R) (2014).
- [18] N. Locatelli, A. Hamadeh, F. A. Araujo, A. D. Belanovsky, P. N. Skirdkov, R. Lebrun, V. V. Naletov, K. A. Zvezdin, M. Muñoz, J. Grollier, O. Klein, V. Cros, and G. de Loubens, Efficient synchronization of dipolarly coupled vortex-based spin transfer nano-oscillators, *Sci. Rep.* **5**, 17039 (2015).
- [19] A. D. Belanovsky, N. Locatelli, P. N. Skirdkov, F. A. Araujo, K. A. Zvezdin, J. Grollier, V. Cros, and A. K. Zvezdin, Numerical and analytical investigation of the synchronization of dipolarly coupled vortex spin-torque nano-oscillators, *Appl. Phys. Lett.* **103**, 122405 (2013).
- [20] A. V. Sadovnikov, A. A. Zyablovsky, A. V. Dorofeenko, and S. A. Nikitov, Exceptional-point phase transition in

- coupled magnonic waveguides, *Phys. Rev. Appl.* **18**, 024073 (2022).
- [21] O. S. Temnaya, A. R. Safin, D. V. Kalyabin, and S. A. Nikitov, Parity-time symmetry in planar coupled magnonic heterostructures, *Phys. Rev. Appl.* **18**, 014003 (2022).
- [22] H. M. Hurst and B. Flebus, Non-Hermitian physics in magnetic systems, *J. Appl. Phys.* **132**, 220902 (2022).
- [23] S. Wittrock, S. Perna, R. Lebrun, K. Ho, R. Dutra, R. Ferreira, P. Bortolotti, C. Serpico, and V. Cros, Non-hermiticity in spintronics: Oscillation death in coupled spintronic nano-oscillators through emerging exceptional points, [arXiv:2108.04804v2](https://arxiv.org/abs/2108.04804v2).
- [24] I. V. Doronin, A. A. Zyablovsky, E. S. Andrianov, A. A. Pukhov, and A. P. Vinogradov, Lasing without inversion due to parametric instability of the laser near the exceptional point, *Phys. Rev. A* **100**, 021801(R) (2019).
- [25] J. Wiersig, Prospects and fundamental limits in exceptional point-based sensing, *Nat. Commun.* **11**, 2454 (2020).
- [26] J. Wiersig, Review of exceptional point-based sensors, *Photonics Res.* **8**, 1457 (2020).
- [27] X.-g. Wang, G.-h. Guo, and J. Berakdar, Steering magnonic dynamics and permeability at exceptional points in a parity-time symmetric waveguide, *Nat. Commun.* **11**, 5663 (2020).
- [28] P. Bortolotti, E. Grimaldi, A. Dussaux, J. Grollier, V. Cros, C. Serpico, K. Yakushiji, A. Fukushima, H. Kubota, R. Matsumoto, and S. Yuasa, Parametric excitation of magnetic vortex gyrations in spin-torque nano-oscillators, *Phys. Rev. B* **88**, 174417 (2013).
- [29] K. Y. Guslienko, Magnetic vortex state stability, reversal and dynamics in restricted geometries, *J. Nanosci. Nanotechnol.* **8**, 2745 (2008).
- [30] A. Dussaux, B. Georges, J. Grollier, V. Cros, A. Khvalkovskiy, A. Fukushima, M. Konoto, H. Kubota, K. Yakushiji, S. Yuasa, K. A. Zvezdin, K. Ando, and A. Fert, Large microwave generation from current-driven magnetic vortex oscillators in magnetic tunnel junctions, *Nat. Commun.* **1**, 8 (2010).
- [31] K. S. Buchanan, P. E. Roy, M. Grimsditch, F. Y. Fradin, K. Y. Guslienko, S. D. Bader, and V. Novosad, Magnetic-field tunability of the vortex translational mode in micron-sized permalloy ellipses: Experiment and micromagnetic modeling, *Phys. Rev. B* **74**, 064404 (2006).
- [32] A. A. Thiele, Applications of the gyrocoupling vector and dissipation dyadic in the dynamics of magnetic domains, *J. Appl. Phys.* **45**, 377 (1974).
- [33] Z. Liu, F. Giesen, X. Zhu, R. D. Sydora, and M. R. Freeman, Spin wave dynamics and the determination of intrinsic damping in locally excited permalloy thin films, *Phys. Rev. Lett.* **98**, 087201 (2007).
- [34] B. Krüger, A. Drews, M. Bolte, U. Merkt, D. Pfannkuche, and G. Meier, Harmonic oscillator model for current- and field-driven magnetic vortices, *Phys. Rev. B* **76**, 224426 (2007).
- [35] K. L. Metlov and K. Y. Guslienko, Stability of magnetic vortex in soft magnetic nano-sized circular cylinder, *J. Magn. Magn. Mater.* **242-245**, 1015 (2002).
- [36] M. Bolte, G. Meier, B. Krüger, A. Drews, R. Eiselt, L. Bocklage, S. Bohlens, T. Tylliszczak, A. Vansteenkiste, B. Van Waeyenberge, K. W. Chou, A. Puzic, and H. Stoll, Time-resolved x-ray microscopy of spin-torque-induced magnetic vortex gyration, *Phys. Rev. Lett.* **100**, 176601 (2008).
- [37] J. Shibata, K. Shigeto, and Y. Otani, Dynamics of magnetostatically coupled vortices in magnetic nanodisks, *Phys. Rev. B* **67**, 224404 (2003).
- [38] C. Hayashi, *Nonlinear Oscillations in Physical Systems* (Princeton University Press, 2014), Chap. 3, pp. 92–95.